Structural Studies on Phospho-CDK2/Cyclin A Bound to Nitrate, a Transition State Analogue: Implications for the Protein Kinase Mechanism†,‡

A. Cook,§ E. D. Lowe,§ E. D. Chrysina,|| V. T. Skamnaki,|| N. G. Oikonomakos,|| and L. N. Johnson*,§

Laboratory of Molecular Biophysics, Department of Biochemistry, University of Oxford, Rex Richards Building, South Parks Road, Oxford OX1 3QU, U.K., and Institute of Biological Research and Biotechnology, The National Hellenic Research Foundation, 48 Vas. Constantinou Avenue, Athens 11635, Greece

Received February 28, 2002; Revised Manuscript Received April 15, 2002

ABSTRACT: Eukaryotic protein kinases catalyze the phosphoryl transfer of the γ-phosphate of ATP to the serine, threonine, or tyrosine residue of protein substrates. The catalytic mechanism of phospho-CDK2/cyclin A (pCDK2/cyclin A) has been probed with structural and kinetic studies using the trigonal NO_3^- ion, which can be viewed as a mimic of the metaphosphate transition state. The crystal structure of pCDK2/cyclin A in complex with Mg^{2+}ADP, nitrate, and a heptapeptide substrate has been determined at 2.7 Å. The nitrate ion is located between the β-phosphate of ADP and the hydroxyl group of the serine residue of the substrate. In one molecule of the asymmetric unit, the nitrate is close to the β-phosphate of ADP (distance from the nitrate nitrogen to the nearest β-phosphate oxygen of 2.5 Å), while in the other subunit, the nitrate is closer to the substrate serine (distance of 2.1 Å). Kinetic studies demonstrate that nitrate is not an effective inhibitor of protein kinases, consistent with the structural results that show the nitrate ion makes few stabilizing interactions with CDK2 at the catalytic site. The binding of orthovanadate was also investigated as a mimic of a pentavalent phosphorane intermediate of an associative mechanism for phosphoryl transfer. No vanadate was observed bound in a 3.4 Å resolution structure of pCDK2/cyclin A in the presence of Mg^{2+}ADP, and vanadate did not inhibit the kinase reaction. The results support the notion that the protein kinase reaction proceeds through a mostly dissociative mechanism with a trigonal planar metaphosphate intermediate rather than an associative mechanism that involves a pentavalent phosphorane intermediate.

The cyclin-dependent protein kinase, CDK2, regulates the eukaryotic cell cycle at the G1−S boundary and during the S phase in which nuclear DNA is replicated. The tight regulation ensures that DNA is replicated once and only once and also ensures that mitosis does not occur until replication has been completed. Cell cycle regulation is dependent upon the activation and deactivation of CDKs and their selective phosphorylation of downstream target proteins. To become active, CDK2 requires association with a cyclin (cyclin E at the G1−S phase transition and cyclin A during the S phase) and phosphorylation of a threonine residue (Thr160) in the so-called kinase activation segment (*1*). The activity may be inhibited by protein inhibitors of the $p27^{Kip1}$ family and by further phosphorylation on a threonine (Thr14) and a tyrosine (Tyr15) in the kinase glycine rich loop. Because of the biological importance of CDK2, there is a major effort with structural, cellular, and kinetic studies to understand the basis of regulation, the substrate selectivity, and the catalytic mechanism.

CDK2 is a member of the eukaryotic protein kinase family that catalyzes the phosphoryl transfer of the γ-phosphate of ATP to the hydroxyl of a serine, threonine, or tyrosine residue in the protein substrate. Phosphorylation of the target protein can have dramatic downstream consequences, leading to conformational response, activation or inhibition of catalytic activity, association or dissociation of complexes, and translocation to different cell compartments (*2*). The eukaryotic protein kinase superfamily is the third largest in the human genome and represents ~2% of the genome. The protein kinases play critical roles in cell signaling pathways and have become important targets in drug design for treatment of a number of pathological conditions, including cancer (*3*). The structures of more than 30 protein kinases determined to date by X-ray diffraction studies show that they all share a common fold comprising an N-terminal domain largely composed of β-sheet with one helix, the C helix, whose correct orientation is important for catalysis, and a larger C-terminal domain composed of mostly α-helices. The catalytic site is at the domain interface with residues important for ATP binding contributed from both domains and residues important for substrate peptide binding located almost exclusively in the C-terminal domain. The kinases show conservation of Mg^{2+}ATP binding residues and diversity in residues that contribute to substrate specificity. Within this common fold, the kinases display a variety of different mechanisms for regulation, but once activated, the

† This work was supported by the MRC and BBSRC, a Wellcome Trust Biomedical Research Collaboration grant, and a Royal Society Joint Project Grant (to L.N.J. and N.G.O.).

‡ Coordinates have been deposited as Protein Data Bank entry 1gy3.

* To whom correspondence should be addressed. Telephone: 44-(0)1865 275365. Fax: 44-(0)1865 510454. E-mail: louise@biop.ox.ac.uk.

§ University of Oxford.

|| The National Hellenic Research Foundation.

10.1021/bi0201724 CCC: $22.00
Published on Web 05/15/2002

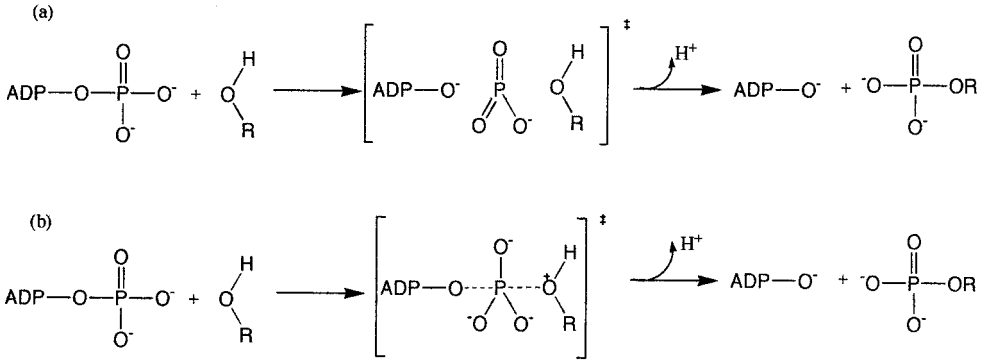

FIGURE 1: Schematic representation of the dissociative and associative extremes for phosphoryl transfer. (a) The dissociative mechanism proceeds through a metaphosphate intermediate transition state (in which the actual nature of bonding in the metaphosphate-like species is uncertain) and the absence of bonds to the incoming and outgoing groups. (b) The associative mechanism proceeds through a pentavalent transition state in which the incoming group has substantial bond formation before the leaving group has left. In the dissociative mechanism, there is accumulation of charge on the phosphoryl oxygen that links the β- and γ-phosphate groups of ATP. In the associative mechanism, there is an accumulation of charge on the peripheral oxygens of the departing γ-phosphate (adapted from ref *16*).

key residues at the catalytic site are highly conserved both in amino acid sequence and in their spatial positions, an observation that suggests that eukaryotic protein kinases share a common mechanism for phosphoryl transfer.

Studies on four protein kinases [cyclic AMP-dependent protein kinase (cAPK) (*4*, *5*), insulin receptor tyrosine kinase (IRK) (*6*), phosphorylase kinase (PhKγtrnc) (*7*), and phosphoThr160-CDK2/cyclin A (pCDK2[1]/cyclin A) (*8*)] in ternary complex with inactive ATP analogues and peptide substrate or substrate mimics have shown the importance of the correct alignment of the ATP and peptide substrate in facilitating phosphoryl transfer. Critical for the alignment of the ATP triphosphate moiety is the correct positioning of a lysine (Lys33 in CDK2) through contact with a glutamate (Glu51) from the C helix of the kinase, which reorients in response to activation. The crucial part of the peptide substrate alignment comes from interactions of the substrate with the activation segment, a part of the kinase chain from the conserved DFG motif (residues 145−147 in CDK2) and the APE motif (residues 172−175 in CDK2). The activation segment carries the phosphorylated residue(s) (Thr160 in CDK2) in three of the four kinases whose ternary complex structures are known, and phosphorylation plays a critical role in promoting the correct alignment of this part of the chain. In the fourth example, the kinase domain of phosphorylase kinase [PhKγtrnc (*7*)], the activation segment adopts the correct conformation without the need for external phosphorylation, and a glutamate (Glu182) occupies the position taken by the phosphoryl residue. Structural studies have demonstrated the subtle conformational changes localized to the activation segment on transition from the low-activity CDK2/cyclin A complex to the high-activity pCDK2/cyclin A complex (*9*, *10*). These conformational changes create the correct substrate recognition pocket that defines the specificity for the Ser-Pro motif of the substrate and the basic group in the P + 3 position (i.e., the residue that is three residues toward the C-terminus from the phosphorylated serine) (*8*). In CDK2, the shift in the activation segment (residues 159−164) upon phosphorylation creates a pocket that can accept the prolyl side chain and only a prolyl side chain, while the substrate basic group (a lysine) contacts the Thr160 phosphate.

Once the complex is in the correctly activated conformation, kinetic studies have shown that the chemical phosphoryl transfer is rapid and the rate-limiting step is release of product. In the pCDK2/cyclin A complex, the chemical step is characterized by a rate constant of 22 s^{-1} and the release of product with a rate constant of 11 s^{-1} (*11*). For cAPK (*12*, *13*) and PhKγtrnc (*14*), the chemical step is considerably faster (500 and >360 s^{-1}, respectively), while the rates for release of product are 20 and 28 s^{-1}, respectively. Interactions between CDK2 and a substrate mimetic peptide in the X-ray crystal structure of pCDK2/cyclin A in complex with the inactive ATP analogue, Mg^{2+}AMPPNP (*8*), showed that the serine hydroxyl group of the substrate peptide points toward the terminal γ-phosphate of the AMPPNP (a nonhydrolyzable ATP analogue) poised for attack on the γ-phosphate of the ATP. The serine hydroxyl is held in place by the conserved catalytic aspartate, Asp127, and a lysine residue, Lys129.

As discussed by Knowles (*15*), the mechanisms of phosphotransfer enzymes can have either mainly associative or mainly dissociative character (Figure 1). The dissociative mechanism is an S_N1 mechanism where a trigonal planar metaphosphate species is formed by the breakage of the P−O bond before any significant bond formation during which the substrate hydroxyl is made. The associative mechanism is an S_N2-like mechanism in which the bond between the terminal phosphorus and the substrate hydroxyl group is partially formed before the P−O bond of the ATP is fully broken, leading to a pentacovalent phosphorane species. Dissociative transition states are well established for nonenzymic phosphoryl transfer reactions (*16*, *17*). A dissociative mechanism may be favored in the absence of an enzyme since in the associative mechanism the negative charges on the phosphate nonbridging oxygens are likely to repel an incoming nucleophile. In an enzyme, positively charged groups from the protein or metal ions could favor the pentavalent-like intermediate of the associative mechanism

[1] Abbreviations: pCDK2, phospho(Thr160)cyclin-dependent kinase 2; PhK, glycogen phosphorylase kinase; PhKγtrnc, residues 1−298 of the γ subunit of PhK; GP, rabbit muscle glycogen phosphorylase; GPa, glycogen phosphorylase *a*, the activated phosphorylated form of glycogen phosphorylase; GPb, glycogen phosphorylase *b*, the inactive form of glycogen phosphorylase; Glc-1-P, α-D-glucose 1-phosphate; HBS, Hepes-buffered saline; Hepes, *N*-(2-hydroxyethyl)piperazine-*N*′-2-ethanesulfonic acid; Tris, tris(hydroxymethyl)aminomethane; PEG 8K, polyethylene glycol with a molecular weight of approximately 8000.

and may provide groups which could activate the incoming nucleophile. In a number of structural studies of phosphotransferase systems such as the UMP/CMP kinase (*18*), nucleoside diphosphate kinase (*19*), the F_1-F_0 ATPase (*20*), the ras GTPases (*21*), and arginine kinase (*22*), small trigonal planar molecules such as AlF_3 or NO_3^- have been used to mimic the possible pentacovalent phosphorane or the trigonal planar metaphosphate species. Distances between the aluminum and the leaving group and nucleophilic oxygen were intermediate between van der Waals and covalent bond distances, suggesting that it is possible to discriminate between a mostly associative mechanism (UMP/CMP kinase and $p21^{ras}$), a mostly dissociative mechanism (nucleoside diphosphate kinase), and a hybrid mechanism (arginine kinase). Interactions of substrates with several positively charged groups were typical of the structures proposed to resemble an associative mechanism. In a dissociative mechanism, the importance of the attacking nucleophile is diminished. In studies with two tyrosine kinases in which the nucleophilicity of the attacking hydroxyl of the tyrosine residue was varied, Cole and colleagues have provided evidence for a dissociative metaphosphate-like transition state (*23*, *24*) and have used this information in the design of a potent bis-substrate inhibitor (*25*).

In this study, we have determined the structures of possible transition state analogue complexes with pCDK2/cyclin A. A complex was formed between pCDK2/cyclin A, Mg^{2+}-ADP, nitrate, and a heptapeptide substrate derived from an optimal peptide substrate determined from library screening. We used nitrate in preference to the more widely used AlF_3 or AlF_4 molecules since the coordination number of AlF_x is influenced by pH (*26*). The singly charged NO_3^- ion is closer to the proposed transition state than the neutral AlF_3, while the singly charged square planar AlF_4^- species does not have the right geometry to mimic the transition state. We have also studied the structure of the pCDK2/cyclin A−Mg^{2+}-ADP complex in which the crystals were soaked in vanadate. Orthovanadate is a potent inhibitor of several enzymes that catalyze phosphoryl transfer (*27*). It has proven to be a useful phosphate mimic in reactions that proceed through a covalent phosphoryl intermediate such as protein tyrosine phosphatase 1B (PTP1B) (*28*). The ion can readily adopt a trigonal bipyramidal coordination that has been proposed to mimic the conformation of a pentavalent phosphorane intermediate, as in the studies with ribonuclease (*29*). It is also a potent inhibitor of myosin ATPase, forming a long-lived complex with Mg^{2+}ADP. In structural studies with the myosin ATPase−Mg^{2+}ADP−VO_4 complex, vanadate formed a trigonal bipyramidal coordinated structure in which one apical coordination site was occupied by the terminal oxygen of the β-phosphate of ADP and the other by a water molecule in a structure that with associated protein ligands was proposed to mimic a mainly associative transition state (*30*). We were interested in observing the geometry of the putative transition state complexes in terms of distances between the incoming attacking and leaving oxygens, and in learning if additional positively charged groups enter the catalytic site that could promote stabilization of either an associative or dissociative type transition state, or if there are movements of other side chains whose new positions could enhance the nucleophilicity of the catalytic aspartate.

EXPERIMENTAL PROCEDURES

Human CDK2 phosphorylated on Thr160 (pCDK2) was produced in *Escherichia coli* strain B834(DE3) plysS by coexpression of a human GST−CDK2 conjugate and a *Saccharomyces cerevisiae* GST−Cak1 conjugate as described previously (*8*). Human cyclin A3 (residues 174−432) was also expressed in *E. coli* (*8*). The pCDK2/cyclin A complex was prepared by immobilization of the GST−pCDK2 conjugate on a glutathione-Sepharose column, addition of the cleared cell lysate from cells expressing cyclin A3, elution of the GST−pCDK2/cyclin A complex from the glutathione-Sepharose column with 20 mM glutathione in HBS, and digestion with 3C protease (1/30 w/w, 16 h, 4 °C) to cleave GST from pCDK2. The pCDK2/cyclin A complex was purified by gel filtration (Superdex75 HR26/60 column) followed by a second glutathione-Sepharose column (*8*). The pCDK2/cyclin A complex was concentrated in a Centricon-10 apparatus (Millipore) to 10 mg/mL.

Crystallography. Crystals of pCDK2/cyclin A were grown by the vapor diffusion method using sitting drops at 4 °C from solutions containing 10 mg/mL pCDK2/cyclin A, 100 mM HEPES (pH 7.0), 2 mM substrate peptide HHASPRK, 1 mM ADP, and Li_2SO_4 in a range of concentrations from 1.05 to 1.15 M. Mg^{2+} was not added at this stage because it interferes with crystallization. Previous experience has shown that the peptide substrate binds poorly in the presence of high-ionic strength Li_2SO_4 (*8*). Therefore, the crystals were transferred to a low-ionic strength stabilization buffer containing 20% PEG 8K, 100 mM HEPES (pH 7.0), and 10 mM substrate peptide, to increase the level of substrate peptide binding, and 5 mM $Mg(NO_3)_2$, to introduce both Mg^{2+} and NO_3^- into the crystals. The soak time was 2 h. Crystals were cryoprotected in a stabilization buffer solution containing 20% glycerol before being frozen.

Data to 2.7 Å resolution were collected at the ID14.1 beamline at the ESRF (Grenoble, France) with a CCD detector using an oscillation angle of 0.5° and a total ϕ angle range of 71°. Data were processed using MOSFLM, SCALA, and programs from the CCP4 suite (*31*). The crystals are in space group $P2_12_12$ with two pCDK2/cyclin A molecules in the asymmetric unit related by a noncrystallographic 2-fold axis parallel to the crystallographic *c* axis. The structure was determined by rigid body refinement in REFMAC (*32*) using data of increasing resolution and rigid bodies of decreasing size with the starting model of the isomorphous structure of pCDK2/cyclin A in complex with Mg^{2+}AMPPNP and peptide substrate (PDB entry 1qmz) (*8*), from which the Mg^{2+}AMPPNP and water molecules had been removed. The structure was refined with maximum likelihood refinement in REFMAC with weighting of 0.05 for X-ray to stereochemical restraints. After five cycles, SIGMA-A-weighted (*33*) $2F_o - F_c$ and $F_o - F_c$ electron density maps indicated the positions of Mg^{2+}ADP, nitrate, and two glycerol molecules which were built using the molecular graphics package O (*34*). Further refinement continued with iterative rebuilding in O. Water molecules were included using REFMAC/ARP (*35*). The data collection and refinement statistics are summarized in Table 1.

To determine if the peptide substrate was important for nitrate binding, crystals were grown in the presence of 2 mM peptide, 1 mM ADP, and Li_2SO_4 as described above and

Table 1: Crystallographic Data and Refinement Statistics

	pCDK2/cyclin A−Mg^{2+}ADP−nitrate−peptide substrate	pCDK2/cyclin A−Mg^{2+}ADP−nitrate[a]	pCDK2/cyclin A−Mg^{2+}ADP−vanadate[a]
	Data Collection		
synchrotron source	14.2 ESRF	Elettra	14.2, SRS
space group	$P2_12_12$	$P2_12_12$	$P2_12_12_1$
cell dimensions (Å)	$a = 150.71$, $b = 164.10$, $c = 72.43$	$a = 150.79$, $b = 164.68$, $c = 73.42$	$a = 73.25$, $b = 132.44$, $c = 147.31$
maximum resolution (Å)	2.7 (2.81−2.7)	2.2	3.4
no. of observations	319218	279836	36708
no. of unique reflections	45572	93364	20937
R_{merge}[b] (%)	14.3 (48.7)	12.9 (45.1)	12.6 (34.7)
completeness (%)	84.4 (40.7)	97.4 (93.3)	89.3 (93.1)
$I/\sigma(I)$	4.2 (1.5)	4.6 (2.0)	5.6 (2.1)
	Refinement		
no. of atoms	9286	9122	8933
ligands	2 Mg^{2+}, 2 ADP, 2 NO_3, 2 glycerol, 163 H_2O	2 Mg^{2+}, 2 ADP	2 ADP
resolution range (Å)	20−2.7	30−2.2	35−3.4
R_{conv}[c]	0.250	0.285	0.254
R_{free}[c]	0.313	0.308	0.299
mean protein main chain *B* factors (Å^2)	36 for chain A, 32 for chain B, 35 for chain C, 30 for chain D		
mean peptide, Mg^{2+}ADP, NO_3, glycerol, and water temperature factors (Å^2)	58 for chain E, 57 for chain F, 55 for Mg^{2+}ADP (2), 55 for NO_3 (2), 40 for glycerol (2), 30 for waters (162)		
rmsd for bond lengths (Å)	0.020		
rmsd for bond angles (deg)	2.0		

[a] Refinement terminated because relevant ligand not bound. [b] $R_{merge} = (\sum_h\sum_j|I_{h,j} - I_h|)/(\sum_h\sum_j|I_{h,j}|)$, where $I_{h,j}$ is the intensity of the *j*th observation of unique reflection *h*. [c] $R_{conv} = (\sum_h||F_{oh}| - |F_{ch}||)/(\sum_h|F_{oh}|)$, where F_{oh} and F_{ch} are the observed and calculated structure factor amplitudes, respectively, for reflection *h*. R_{free} is equivalent to R_{conv}, but is calculated using a 5% disjoint set of reflections excluded from the least-squares refinement stages.

then soaked in the same well buffer containing 5 mM $Mg(NO_3)_2$ and 2 mM ADP for 2 h. Crystals were cryoprotected with 20% glycerol as described above. Data for these crystals were collected at the Elettra synchrotron (Trieste, Italy) to 2.2 Å resolution and processed with MOSFM, SCALA, and CCP4. The structure was determined as described above (Table 1). Electron density maps after refinement with REFMAC indicated positions of Mg^{2+}ADP binding but no evidence for nitrate binding in either of the two molecules in the asymmetric unit. There was a weak indication of the Ser and Pro residues of the peptide substrate at the A subunit CDK2 kinase catalytic site. The refinement of this structure was not completed in view of the negative result.

To examine vanadate binding, crystals of pCDK2/cyclin A were obtained by the sitting drop method using protein at a concentration of 10 mg/mL in 10 mM HEPES (pH 7.5) containing 1 mM AMPPNP, 3 mM EDTA, 0.01% (v/v) monothioglycerol, and 150 mM NaCl at 4 °C. The reservoir solution contained 0.7−0.8 M KCl and 1.0−1.1 M $(NH_4)_2SO_4$ in 100 mM HEPES (pH 7.0). The crystals grown in the presence of $(NH_4)_2SO_4$ are chunkier and more robust than the thin platelike crystals grown in the presence of Li_2SO_4, and for this reason, they were considered more suitable for soaks in the potentially damaging vanadate solutions. The crystals belong to space group $P2_12_12_1$ with two molecules per asymmetric unit. AMPPNP was removed by soaking the crystals in the reservoir solution in the absence of nucleotide for 1 h. Crystals were then soaked in 2 mM ADP for 1 h followed by a soak in 2 mM ADP, 2 mM sodium vanadate, and 5 mM $MgCl_2$ in reservoir solution for 12 h. The peptide substrate was omitted from these crystals because it was anticipated that, if bound, the apical positions of the vanadate would be occupied by an oxygen from ADP and either the fourth oxygen of the VO_4 ion or a water as in myosin ATPase. The crystals were cryoprotected with 8 M formate. Data were collected on beam line 14.2 at SRS (Daresbury, Warrington, U.K.) using an ADSC Quadra CCD detector. The crystals were small (<0.1 μm in their longest dimension), and data to only 3.4 Å resolution could be recorded. The structure was determined using molecular replacement, rigid body refinement, and refinement with REFMAC with alternate cycles of electron density map examination in O as described above (Table 1). After refinement, ADP was visible at the catalytic site, but there was no evidence of vanadate binding. The refinement was terminated.

Kinetics. The phosphorylation of the peptide substrate HHAPSRK by pCDK2/cyclin A was assessed spectrophotometrically using an assay (*36*, *37*) in which ADP production is coupled through the reaction of the kinase to the NADH oxidation by pyruvate kinase and lactate dehydrogenase, with minor modifications. All reactions were carried out at 30 °C in a total volume of 0.3 mL. The assay mixture contained 2 μg/mL enzyme, 30 units/mL lactate dehydrogenase, 10 units/mL pyruvate kinase, 1 mM phosphoenolpyruvate, 0.3 mM NADH, 0.5 mg/mL bovine serum albumin, 50 mM Hepes (pH 7.5), 150 mM NaCl, 10 mM magnesium acetate, and 2 mM dithiothreitol. The peptide concentration varied from 0.05 to 2.0 mM. The reaction was initiated by the simultaneous addition of pCDK2/cyclin A and 1.0 mM ATP (final concentration). Samples were withdrawn at 0.5 min intervals over the period from 5 to 15 min and transferred into 0.1% sodium dodecyl sulfate (final concentration) to stop the reaction. The NADH consumption in the reaction results in a decrease in absorbance at 340 nm. A molar extinction coefficient of 6220 M^{-1} cm^{-1} for NADH at 340 nm was used in the calculations. Reaction rates varied linearly with the concentration of pCDK2/cyclin A.

PhKγtrnc, residues 1−298 of the γ-subunit of PhK, was prepared as described previously (*38*) with minor modifications. The native enzyme was expressed in BL21DE3 plysS cells as inclusion bodies. The inclusion bodies were denatured by urea, refolded, and purified using anion exchange chromatography on a Q Sepharose (Pharmacia) followed by affinity chromatography on a Cibacron Blue column (Sigma). Glycerol was purchased from Serva. AMP, ATP, glucose 1-phosphate (dipotassium salt), and Hepes were obtained from Sigma. Oyster glycogen (Sigma) was freed of AMP according to the method described in ref *39*. Glycogen phosphorylase *b* (GPb) was isolated from rabbit skeletal muscle according to the method described in ref *40* using 2-mercaptoethanol instead of L-cysteine and recrystallized at least four times. Bound nucleotides were removed from the enzyme as previously described (*41*). The GPb concentration was determined from absorbance measurements at 280 nm using an absorbance index $A^{1\%}{}_{1cm}$ of 13.2 (*42*). PhKγtrnc and pCDK2/cyclin A concentrations were determined according to the method described in ref *43*.

The enzymic activity of PhKγtrnc was measured by monitoring the conversion of GPb to GPa by assaying phosphorylase activity in the presence of 10 μM AMP and 0.5 mM caffeine in the direction of glycogen synthesis (*14*). Reaction mixtures contained, in a volume of 0.2 mL, 50 mM Tris, 50 mM Hepes, 0.5 mM calcium chloride, 10 mM magnesium acetate, 2 mM DTT (pH 8.6), and various concentrations of GPb (1−5 mg/mL) when the assay was performed with respect to GPb at a saturating concentration of ATP (1.0 mM) or various concentrations of ATP (0.05−1.0 mM) at a saturating concentration of GPb (5 mg/mL). After incubation of the reaction mixtures for 1 min at 30 °C, the reaction was initiated by the simultaneous addition of PhKγtrnc and ATP. The concentration of PhKγtrnc was 15−20 ng/mL in the reaction buffer containing BSA (0.5 mg/mL). Samples were withdrawn at 3, 6, and 12 min and diluted by 50-fold in buffer containing 100 mM triethanolamine/HCl (pH 6.8), 1 mM EDTA, and 2 mM DTT at 0 °C. GPa was assayed by assessing the release of orthophosphate from Glc-1-P in a buffer containing 50 mM triethanolamine/HCl, 0.5 mM EDTA, 1 mM DTT, 1% glycogen, 76 mM Glc-1-P, 10 μM AMP, and 0.5 mM caffeine (pH 6.8). The reaction was stopped with sodium dodecyl sulfate at a final concentration of 0.2%. The amount of inorganic phosphate released in the phosphorylase reaction was determined, and initial rate constants were calculated. Kinetic data were analyzed by the use of the nonlinear regression program GRAFIT (*44*). A stock solution of 100 mM sodium orthovanadate (Sigma) (pH 10.0) was prepared as described previously (*45*).

RESULTS

Crystallography. Crystals of the complex of pCDK2/cyclin A with ADP, peptide substrate, and nitrate were achieved by cocrystallization of pCDK2/cyclin A with 1 mM peptide substrate (HHASPRK) and 1 mM ADP with Li_2SO_4 as a precipitant and followed by transfer of the crystals to 20% PEG 8K with 10 mM peptide substrate and 5 mM $Mg(NO_3)_2$ for 2 h. The crystals became fragile after being transferred to the low-ionic strength buffer, which was necessary to improve peptide substrate binding. Several different protocols for the transfer using different PEG concentrations were tried, but none resulted in improvement of the crystals. Data were collected to 2.7 Å (Table 1). The data were only 40% complete in the highest-resolution shell but were 92% complete to a resolution of 2.8 Å. The inclusion of the data to 2.7 Å resolution improved the electron density maps. After rigid body refinement and five cycles of restrained refinement with REFMAC with the starting model of the pCDK2/cyclin A structure with peptide substrate, clear density was visible for the Mg^{2+}ADP and the nitrate ions in both copies of the kinase in the asymmetric unit. In addition, two glycerol molecules were found in the structure. One of these is located in cyclin A (chain B) in a small pocket enclosed by the loop formed by residues 342−349 (the loop between helices $\alpha2'$ and $\alpha3'$ in the second cyclin box fold) and contacting the side chains of Arg211 and Asp240 from helices $\alpha1$ and $\alpha2$, respectively, of the first cyclin box fold. The second glycerol was found at the contact interface between the C chain kinase of one CDK2/cyclin A complex and the B chain cyclin of another CDK2/cyclin A complex. This glycerol hydrogen bonds to the side chains of Asn23, Glu28, and Glu68 and a water of the C chain kinase.

A similar refinement of the structure of pCDK2/cyclin A in which the crystals grown in the presence of peptide substrate and ADP were transferred to 2 mM ADP and 5 mM $Mg(NO_3)_2$ showed binding of ADP, no indication of nitrate binding, and only weak evidence for the Ser and Pro residues of the substrate peptide in the A subunit. The refinement of this structure was terminated before completion in view of the absence of nitrate binding.

Crystals of pCDK2/cyclin A which had been crystallized in the presence of $(NH_4)_2SO_4$ and subsequently soaked in 2 mM ADP, 2 mM vanadate, and 3 mM $MgCl_2$ yielded data to only 3.4 Å resolution because of the small size of the crystals. The structure was determined using molecular replacement, rigid body refinement, and refinement with REFMAC. The electron density maps indicated binding of ADP but no binding of vanadate. The refinement was terminated in view of the negative result.

Analysis of the pCDK2/Cyclin A−Mg^{2+}ADP−Nitrate−Peptide Complex. The two kinase subunits in the asymmetric unit (chains A and C) superimpose with an rms difference in Cα coordinates of 0.34 Å. This difference is within the estimated coordinate error for the structure at 2.7 Å resolution. We had previously determined the structure of pCDK2/cyclin A in complex with Mg^{2+}AMPPNP and the peptide substrate. The rms differences in Cα coordinates between the Mg^{2+}ADP−peptide−nitrate complex and the Mg^{2+}-AMPPNP−peptide complex are 0.44 and 0.42 Å, respectively, for the A and C subunits and indicate little conformational change between the two complexes. The residues that are conserved in all protein kinases (Lys33, Glu51, Asp127, Lys129, Asn132, and Asp145) show only minor differences in their positions. The two molecules in the asymmetric unit allow two independent views of the arrangement of atoms at the catalytic site and reveal similarities and differences in the binding of ligands. A view of the electron density in the vicinity of the two CDK2 catalytic sites is shown in Figure 2. As indicated by the electron density, the nitrate is closer to the ADP in the A subunit and closer to the peptide serine in the C subunit.

Figure 3 shows the contacts made at the catalytic site in the pCDK2/cyclin A−Mg^{2+}AMPPNP−peptide complex (*8*)

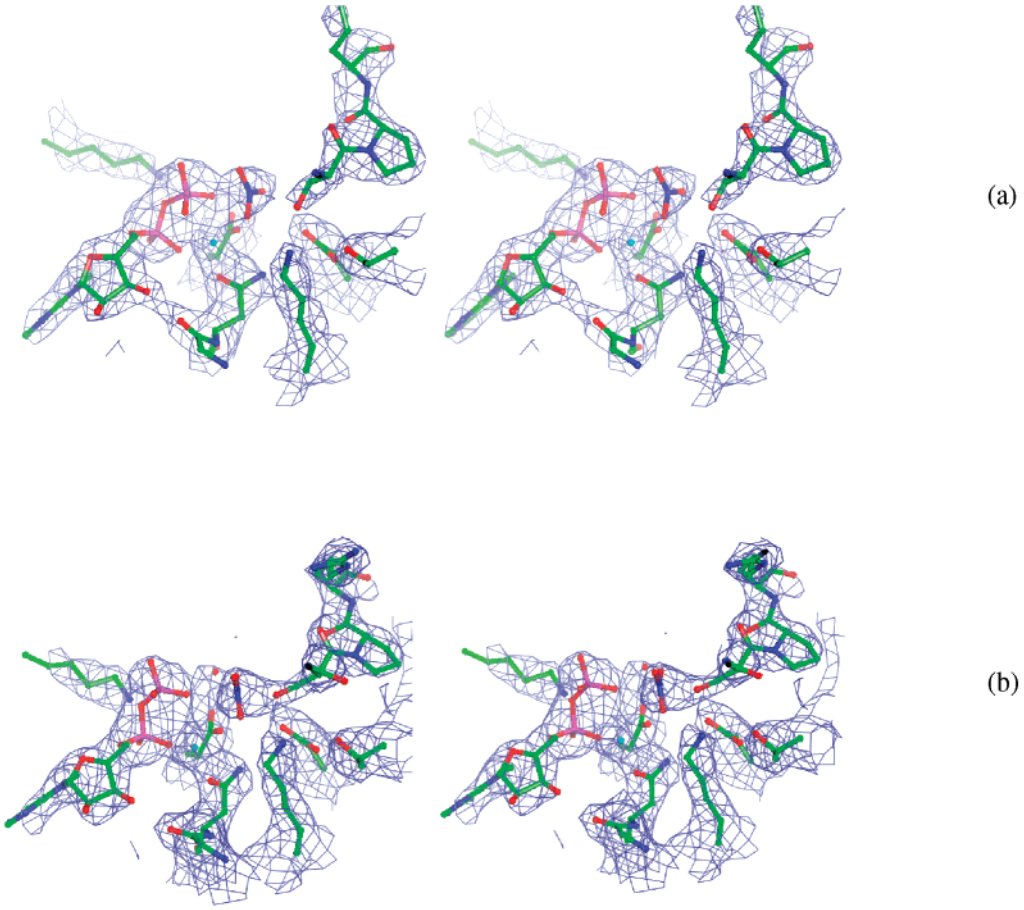

FIGURE 2: Stereoviews of the electron density map (SigmaA-weighted $2F_o - F_c$) in the vicinity of the catalytic site of CDK2 contoured at a level corresponding to 1σ. (a) A subunit. (b) C subunit. ADP is shown at the left and the part of the peptide substrate Ser-Pro-Arg to the right. Nitrate is shown bound at the center of the figure. In the A subunit, nitrate is closer to ADP, and in the C subunit, it is closer to the peptide serine. This figure was produced with AESOP (M. E. M. Noble, unpublished work).

and in the two subunits of the present pCDK2/cyclin A−Mg^{2+}ADP−nitrate−peptide complexes. The essential contacts for the pCDK2/cyclin A−Mg^{2+}AMPPNP−peptide complex have already been described (*8*). In brief (Figure 3a), the triphosphate moiety of AMPPNP is located through contacts to Lys33 and the Mg^{2+} ion. The Mg^{2+} ion contacts the α and γ nonbridging phosphate oxygens, the $\beta-\gamma$ bridging phosphate oxygen, the side chain atoms of Asn132 and Asp145, and a water molecule. It is six-coordinate with octahedral symmetry. The serine of the peptide substrate is hydrogen bonded to one of the peripheral γ-phosphate oxygens, to Asp127, the catalytic aspartate, and to the conserved lysine, Lys129. A network of hydrogen bonds links Asp127 to Asn132 through the Mg^{2+} ion to Asp145. The network is enhanced by three water molecules. The structure, determined at 2.1 Å resolution, had 763 water molecules incorporated. In the new structure of the pCDK2/cyclin A−Mg^{2+}ADP−nitrate−peptide complex at 2.7 Å resolution, only 162 water molecules have been added. The lack of water molecules at the catalytic site in this work is due to the more cautious approach necessitated by the lower resolution.

In the pCDK2/cyclin A−Mg^{2+}ADP−nitrate−peptide complex, ADP is located at the nucleotide binding site. The adenine moiety makes characteristic hydrogen bonds between the adenine N6 and N1 atoms and the hinge region main chain atoms of Glu81 (O) and Leu83 (N), respectively, while the ribose O2′ and O3′ hydroxyls make hydrogen bonds to the Asp86 side chain and Gln131 O, respectively, as also observed in the pCDK2/cyclin A−Mg^{2+}AMMPPNP−peptide complex (details not shown). The α- and β-phosphates are in slightly different conformations in the two subunits, resulting in the difference in position in the β-phosphorus atoms of 0.7 Å after superposition of the two kinase subunits. Consequently, the β-phosphate interactions are slightly different (panels b and c of Figure 3). Both phosphates are stabilized by contacts from Lys33 NZ to the $\alpha-\beta$ bridging oxygen, by contacts from the Mg^{2+} ion to the nonbridging oxygens of the α- and β-phosphates, and interactions with the side chains of Asp145, which in the C subunit is mediated by a water molecule. The glycine rich loop (not shown) is displaced between 0.5 and 1.0 Å in the region of Glu12 from its position in the AMPPNP−peptide substrate complex. The main chain nitrogens of this region do not form any interactions with the ADP. In both subunits, the Mg^{2+} ion is chelated by one β-phosphate oxygen, one α-phosphate oxygen, one nitrate oxygen, and the OD2 oxygens of the Asp145 and Asn132 side chains. The coordination of the Mg^{2+} by the five oxygens resembles octahedral coordination in which the sixth site is exposed to the solvent and could be filled by a water molecule, as seen in the AMPPNP−peptide complex (Figure 3a). The Mg^{2+} positions differ by 0.5 Å in the two subunits, a difference that is associated with the difference in the positions of the ADP β-phosphates.

The peptide substrate forms interactions similar to those previously described in the AMPPNP−peptide complex

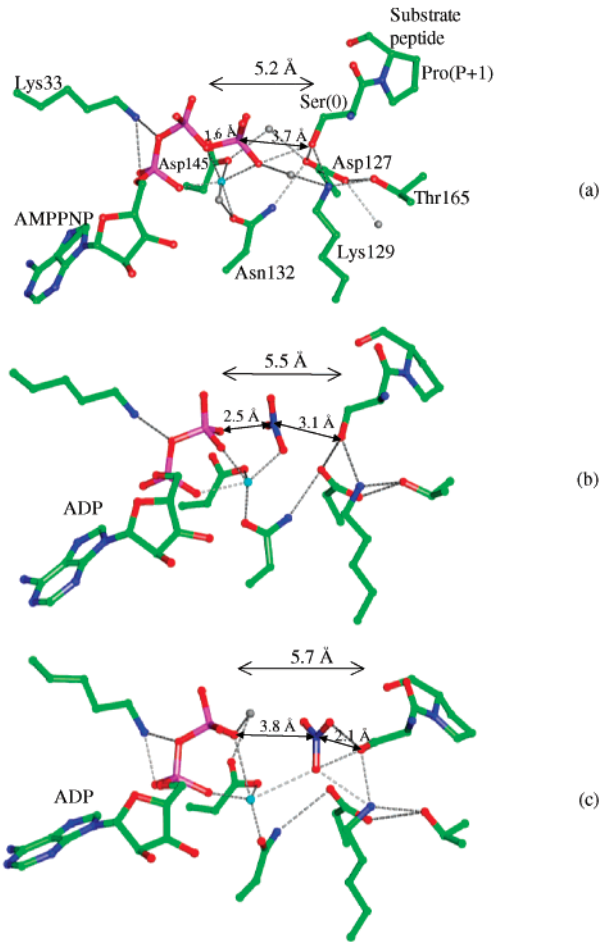

FIGURE 3: Polar contacts at the catalytic site of CDK2 in complex with substrates and substrate analogues. (a) Complex of pCDK2/cyclin A with Mg^{2+}AMPPNP and substrate peptide from ref *8*. (b) Complex of pCDK2/cyclin A with Mg^{2+}ADP, nitrate, and peptide substrate at the A subunit. (c) Complex of CDK2/cyclin A with Mg^{2+}ADP, nitrate, and peptide substrate at the C subunit. Water molecules are shown in gray. More water molecules were identified in the 2.1 Å structure of ref *8* than in the present work at 2.7 Å resolution. Mg^{2+} is shown in cyan. AMPPNP or ADP is shown at the left. The substrate peptide Ser-Pro is shown at the right. Nitrate is shown in the center in panels b and c. The view in panel c is slightly different from that in panels a and b to show a water molecule. This figure was produced with AESOP (M. E. M. Noble, unpublished work).

structure (*8*). The proline in the P + 1 site docks into a pocket created by residues of the activation segment in the region of residues 162−165. In the kinase A subunit, the C-terminal lysine at the P + 3 site is poorly ordered, although it has refined, like the better ordered residue at the kinase C subunit, to contact the Thr160 phosphate.

The nitrate ion is located between the OG atom of the peptide substrate serine at P0 and the β-phosphate of ADP (Figures 2 and 3). The positions differ significantly in the two subunits (by ~2 Å in the positions of the nitrate nitrogen atoms). In the A subunit, the nitrate is closer to the β-phosphate of the ADP, and in the C subunit, it is closer to the OG atom of the peptide serine. The distances from the nitrate nitrogen to the β-phosphate oxygen O1B are 2.5 and 3.8 Å in the A and C subunits, respectively. The distances from the nitrate nitrogen atom to the serine hydroxyl group are 3.1 and 2.1 Å in the A and C subunits, respectively (panels b and c of Figure 3). In both subunits, the nitrate is held in the catalytic site by relatively few contacts. In the A subunit, one nitrate oxygen atom contacts the Mg^{2+} atom and the OD2 atom of Asp145, and there are slightly longer contacts to a β-phosphate oxygen of ADP and the OG atom of the peptide serine. A second nitrate oxygen contacts Asp145 OD2 and a β-phosphate oxygen. The third nitrate oxygen contacts two β-phosphate oxygens. In the C subunit, two nitrate oxygens contact the peptide Ser OG atom. In addition, one oxygen contacts the Mg^{2+} ion and the NZ atom of Lys129, and a second oxygen contacts a β-phosphate oxygen. In both subunits, the catalytic aspartate, Asp127, which is conserved in all protein kinases, is linked through hydrogen bonds from its OD2 atom to the ND2 atom of Asn132 and from its OD1 atom to the OG atom of Thr165 which in turn is hydrogen bonded to the NZ atom of Lys129 (Figure 3). Lys129 NZ is also hydrogen bonded to the OG atom of the peptide serine. In the A subunit, serine OG contacts Asp127 OD2, but in the C subunit, the distance is just too long (3.6 Å) for a hydrogen bond. The peptide substrate is slightly displaced away from the position that is observed for the peptide in the AMPPNP−peptide complex. There is a shift of ~0.5 Å in the Cα positions of the serine. Overall, there is a greater displacement of the C subunit peptide resulting in a shift of the OG atom of the serine by ~1 Å away from the catalytic site relative to its position in the AMPPNP−peptide complex.

In the AMPPNP−peptide complex, the distance from the $\beta-\gamma$ bridging oxygen to the γ-phosphorus is 1.6 Å, the covalent bond distance, and the distance from the phosphorus to the OG atom of the peptide serine is 3.8 Å (Figure 3a). As expected, the position of the nitrate ion is different from that of the covalently bonded γ-phosphate of AMPPNP. The overall separation between the β-phosphate oxygen and peptide serine OG varies just slightly in the three views of the catalytic site [5.2, 5.5, and 5.7 Å (Figure 3)]. The distances between P of the γ-phosphate in the AMPPNP−peptide complex and the N of the nitrate in aligned structures of the ADP−nitrate−peptide complex are 2.1 and 1.8 Å for the A and C subunits, respectively, with the nitrate being closer to OG of the peptide serine in the C subunit.

Kinetics. The kinetic constants of the pCDK2/cyclin A complex with respect to the peptide HHAPSRK are as follows. The enzyme exhibits a V_{max} value of 10.5 μmol min mg^{-1} (k_{cat} = 13 s^{-1}) and a K_m value of 320 μM for this peptide. Hagopian et al. (*11*) found a k_{cat} value of 7 s^{-1} and a K_m value of 8 μM with the histone H1-derived peptide PKTPKKAKKL. The corresponding values for PhKγtrnc with respect to the peptide RQMSFRL were as follows: k_{cat} = 7.5 s^{-1} and K_m = 257 mM (*7*, *14*).

Nitrate [$Mg(NO_3)_2$] had no effect on the enzymic activity of the pCDK2/cyclin A complex when added in concentrations in the range of 0.5−5 mM, in the presence of 0.1 mM peptide, and ATP concentrations in the range of 0.05−0.2 mM. The results indicate that nitrate is unable to compete with ATP. If it is assumed that ATP has a K_m value of ~55 μM (*11*), then even at 100 times that concentration (5 mM) nitrate does not affect ATP binding. This would be consistent with the crystallographic results which show that nitrate makes relatively few stabilizing interactions with the protein in contrast to ATP which makes many contacts from the adenine and ribose in addition to those from the phosphates.

To investigate if ADP with nitrate is a better inhibitor than nitrate alone, we carried out kinetic studies with PhKγtrnc at constant concentrations of ATP and substrate glycogen phosphorylase and varied concentrations of nitrate in the absence or presence of ADP. These experiments were easier to perform with PhKγtrnc than with pCDK2/cyclin A. Kinetic experiments showed that ADP (0.2, 0.4, and 0.6 mM) is a potent inhibitor of the enzyme with a K_i value of 52 μM with respect to ATP (varied from 0.05 to 1.0 mM) and a constant concentration of GPb (5 mg/mL). Nitrate, when added at concentrations of 1−20 mM, did not affect significantly enzyme activity with respect to ATP, in agreement with the results for the pCDK2/cyclin A complex. In addition, no synergistic inhibition of PhKγtrnc was observed with ADP and varying nitrate concentrations.

Similarly, vanadate (Na_3VO_4), when tested at concentrations of 5−10 mM, with respect to ATP (0.05−1.0 mM) and constant concentration of ADP (0.2 mM) and GPb (5 mg/mL), had no significant effect on the enzymic activity of PhKγtrnc in the absence or presence of ADP.

DISCUSSION

The structure of the pCDK2/cyclin A−Mg^{2+}ADP−nitrate−peptide complex presented here represents a possible transition state analogue complex of a protein kinase. The nitrate ion binds between the hydroxyl group of the substrate serine and the β-phosphate of the ADP. The complex illustrates the fact that the kinase catalytic site can accommodate a small trigonal planar species between the nucleotide diphosphate and the peptide substrate in an orientation that would be expected from an in-line phosphoryl transfer reaction. In the absence of the peptide substrate (but in the presence of 1 M Li_2SO_4), no nitrate is bound. This result suggests that the substrate serine contributes to the formation of the binding site, although it is just possible that the Li_2SO_4 had prevented binding. The crystallographic results show few positively charged contacts between the NO_3^- ion and the protein and indicate that the trigonal ion is not tightly bound. The kinetic results showed that nitrate failed to act as a competitive inhibitor with respect to ATP with pCDK2/cyclin A and with PhKγtrnc and that, with PhKγtrnc, nitrate failed to confer any additional inhibition over and above that observed with ADP alone. The kinetic results indicate that nitrate exhibits weak binding compared with ADP and ATP, consistent with the few contacts seen in the crystal structure. Moreover, there are no movements of positively charged groups in the protein that could result in stabilization of a putative transition state analogue complex as might be expected for an associative mechanism for phosphoryl transfer. Vanadate, which is capable of five-coordinate trigonal bipyramidal geometry, is a potential mimic of such a transition state (*27*). An attempt to bind vanadate to pCDK2/cyclin A in the presence of Mg^{2+}-ADP showed no vanadate binding, and vanadate failed to inhibit PhKγtrnc.

The lack of positively charged contacts for the trigonal ion contrasts with the active sites of other phosphotransferases and ATPases where there are several lysine and arginine groups in addition to the nucleotide-coordinating metal ions. For example, in arginine kinase, the transition state complex between kinase, ADP, nitrate, and arginine (*22*) showed a structure consistent with a hybrid of a dissociative metaphosphate intermediate and an associative (20%) pentavalent γ-phosphate transition state. The nitrate and phosphates of ADP were held in place by a dense network of interactions that included five arginines. The absence of positive charges recruited to the active site of CDK2 and the limited number of contacts made by the nitrate ion to the rest of the protein suggest that catalysis in protein kinases is mostly driven by bringing the reactant molecules together in their correct orientation for phosphoryl transfer rather than by direct complementation of a pentavalent transition state.

The positions of the nitrate ions differ significantly between the A and C CDK2 subunits in the asymmetric unit. In the A subunit, the nitrate is close to the β-phosphate of ADP. The separation between the oxygen of the β-phosphate and N is 2.5 Å compared with the separation of 1.6 Å between the $\beta-\gamma$ bridging oxygen and the γ-phosphorus in AMPPNP (Figure 3). The contacts at the A subunit for the nitrate ion are very similar to those observed for the AMPPNP−peptide complex with the nitrate taking the place of the γ-phosphate of AMPPNP. Thus, in the A subunit, the CDK2−Mg^{2+}ADP−nitrate−peptide complex more closely resembles a state in which the ester bond between Pβ and Pγ has been broken to yield a metaphosphate ion but one in which the ion has not yet moved across to the serine hydroxyl. In contrast, at the C subunit, the nitrate ion is closer to the OG atom of the peptide serine than the ADP. The nitrate nitrogen to serine OG distance is only 2.1 Å, while the separation from the ADP phosphate oxygen has lengthened from 2.5 to 3.8 Å. The structure at 2.7 Å resolution has an estimated coordinate error of ~0.4 Å (based on the free R value and the maximum likelihood estimate). The difference in position (2 Å) of the nitrate between the A and C subunits is significant and is supported by the original difference maps and the final $2F_o - F_c$ electron density maps. The position of the nitrate in the C subunit is consistent with the position of a metaphosphate ion in which the contact from the β-phosphate has lengthened to such an extent that it contributes negligible bond energy and the distance to the serine OG atom allows some covalent character. Fortuitously, in the crystal we appear to have caught a mimic of a metaphosphate in its two extreme states. The paucity of strong interactions that the nitrate ion makes to the kinase allows it to move between these two states. In the A subunit, it is stabilized only by the Mg^{2+} ion, while in the C subunit, it is able to contact Lys129 and the serine hydroxyl.

The constellation of residues seen in the pCDK2/cyclin A−Mg^{2+}ADP−nitrate−peptide complex favors a dissociative mechanism for phosphoryl transfer with a metaphosphate intermediate, rather than an associative mechanism in which the transition state involves a pentacoordinate phosphorane intermediate. The associative mechanism requires a somewhat shorter separation of the entering nucleophilic oxygen and the attacked phosphorus than the dissociative mechanism. Mildvan (*17*) has calculated that a reaction coordinate distance of >4.9 Å between the leaving and attacking oxygen is required for a nonbonded intermediate in a dissociative mechanism, assuming that the only motion during the reaction is that of the [PO_3] moiety. For a pure metaphosphate intermediate, there should be a distance of 6.6 Å for the attacking and leaving oxygen to be within van der Waals

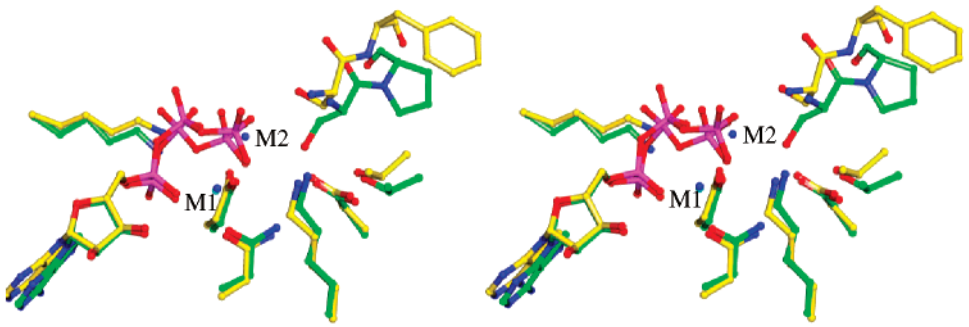

FIGURE 4: Stereodiagram showing a comparison of the catalytic groups in CDK2 (carbon atoms in green) from the ternary enzyme substrate complex described in ref *8* and phosphorylase kinase (carbon atoms in yellow) from the ternary enzyme substrate described in ref *7*. In CDK2, there is only one metal represented at the M1 site (in cyan). In phosphorylase kinase, there are two metals (in blue), one of which (M1) is identical to that in CDK2 and the other of which (M2) bridges the β- and γ-phosphates. This figure was produced with AESOP (M. E. M. Noble, unpublished work).

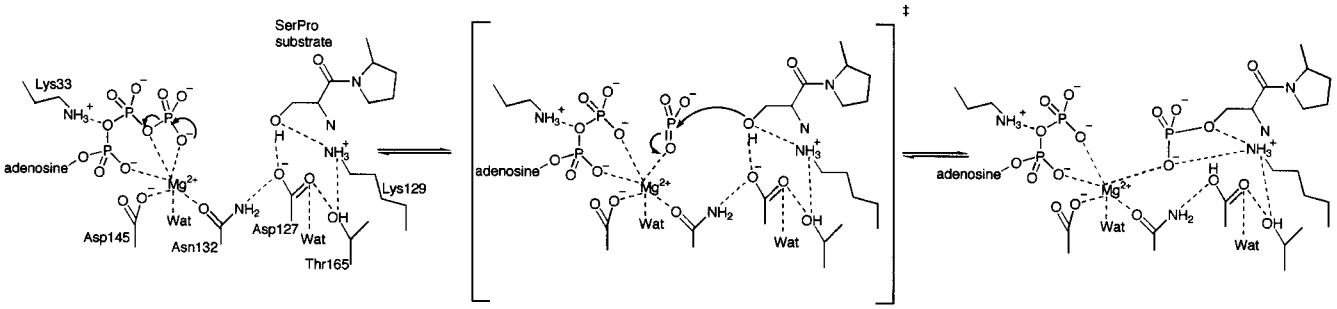

FIGURE 5: Proposals for the catalytic mechanism of pCDK2/cyclin A based on the structures described in the text. Some water molecules seen in the pCDK2/cyclin A−Mg^{2+}AMPPNP−peptide structure have been omitted for clarity. These waters include a water that bridges Asp127 and Asp145 and a water that bridges Lys129 and the γ-phosphate oxygen. For further details, see the text.

contact of the intermediate. For a pure associative mechanism in which the incoming bond is made before the leaving group has left, the distance should be 3.5 Å. Mildvan (*17*) has suggested that the fractional associative character of the reaction may be calculated from the Pauling formula [$D(n) = D(1) - 0.60 \log(n)$, where $D(n)$ is the observed bond distance for the entering group to the phosphorus, $D(1)$ is the phosphorus−oxygen single bond distance (taken to be 1.73 Å), and n is the fractional bond number]. Using the average separation between the incoming and leaving oxygen observed in the substrate and nitrate complexes with pCDK2/cyclin A of 5.5 Å, the fractional associative character of the reaction is calculated to be 2.4%. This value is of course approximate and subject to a number of assumptions described in ref *17*.

A key distinguishing feature between the two mechanisms is the development of charge on the nonbridging oxygens of the γ-pentaphosphoryl intermediate in the associative transition state, while in the dissociative mechanism, there is development of charge on the $\beta-\gamma$ bridging oxygen and only a modest increase in charge on the nonbridging oxygens (Figure 1; *16*). In the dissociative mechanism, the change in charge distribution on going from the ground state to the transition state gives rise to a dipolar distribution in which one side of the transferred phosphoryl group becomes more positive and the other (the bridging oxygen side) more negative. In the pCDK2/cyclin A complexes, the major contribution to the compensation for the buildup of charge on the bridging oxygen is supplied by the Mg^{2+} ion that contacts the bridging atom in the AMPPNP complex and the equivalent atom in the ADP−nitrate complexes. In the A subunit, the nitrate oxygens contact the Mg^{2+} ion and Asp145, while in the C subunit, the nitrate oxygens contact Lys129 and the peptide serine.

Does the catalytic aspartate (Asp127 in CDK2) contribute to catalysis? In previous work, we probed the catalytic mechanism of phosphorylase kinase (Phkγtrnc) through site-directed mutagenesis (*14*). Mutagenesis of Asp149 in Phkγtrnc (equivalent to Asp127 in CDK2) to Asn resulted in a decrease of 4.7×10^3 in k_{cat} compared to that of the wild-type enzyme. It was concluded that a negatively charged group in this position plays a significant role in the chemical step of the reaction. The constellations of catalytic groups at the catalytic sites of CDK2 and Phkγtrnc are essentially identical (Figure 4). In the Phkγtrnc ternary complex, we observed the hydroxyl group of the peptide serine was not directed at the catalytic aspartate, Asp149, but we assumed that during the reaction it would contact the aspartate. In the CDK2 complexes, the peptide serine is directly hydrogen bonded to Asp127. The major difference at the catalytic sites of pCDK2/cyclin A and Phkγtrnc is that in Phkγtrnc there are two metals associated with AMPPNP binding. In Phkγtrnc, one metal (M1 in Figure 4) bridges the α- and γ-phosphates and is in a position identical to that observed in CDK2. The second metal (M2) bridges the β- and γ-phosphates and is not observed in CDK2, despite the presence of 5 mM Mg^{2+} in the soak solution. Previously, we had assumed the second metal bridging the β- and γ-phosphates was the more important one in catalysis following observations on cAPK (*46*−*48*). We now assume that the first metal bridging the α- and γ-phosphates is the more important one for catalysis because it is the only metal present in the CDK2 structure.

We propose a catalytic mechanism outlined in Figure 5. The first and most important step is the correct alignment

of the two substrates, peptide and Mg^{2+}ATP, to favor an in-line mechanism for phosphoryl transfer. The obligatory association of CDK2 with cyclin A results in the correct formation of most of the ATP recognition site, and the obligatory phosphorylation of Thr60 results in the correct formation of the protein or peptide substrate recognition site (*8*, *9*, *11*). With the structure observed in the pCDK2/cyclin A−Mg^{2+}AMPPNP−peptide complex, the lone pair electrons on the peptide serine are directed in-line to the $\beta-\gamma$ bridging atom of the bound nucleoside triphosphate through the phosphorus atom. As the reaction progresses toward the metaphosphate intermediate in a dissociative mechanism, bond breaking of the apical phosphoryl oxygen bond of ATP becomes well advanced while the bond making to the serine hydroxyl is only just beginning. This structure is represented by the pCDK2/cyclin A−Mg^{2+}ADP−nitrate−peptide complex in the A subunit. The development of charge on the phosphoryl oxygen is partly compensated by the Mg^{2+} ion. The acidity of the serine hydroxyl increases as the reaction progresses toward bond formation with the peptide serine. Progress toward bond formation is represented by the pCDK2/cyclin A−Mg^{2+}ADP−nitrate−peptide complex at the C subunit. At the stage before phosphoryl transfer is complete, the pK_a of the seryl hydroxyl will be below that of the carboxyl of Asp127 and proton transfer will occur. In addition, Lys129 is able to stabilize the metaphosphate ion as it approaches the seryl hydroxyl and appears to be an important component of the catalytic machinery. This mechanism would leave Asp127 in a protonated state. The proton could be directly transferred either to the phosphate of the seryl phosphate or to water following release of product.

While this paper was under review, the structure of the cyclic AMP-dependent protein kinase catalytic subunit (cAPK) in complex with Mg^{2+}ADP, aluminum fluoride, and a substrate peptide has been reported at 2 Å resolution (*49*). The AlF_3 molecule is positioned 2.3 Å from both the leaving group oxygen of ADP and the incoming oxygen of the recipient substrate serine residue. The aluminum atom forms a trigonal bipyramidal coordination with the oxygen atoms of the leaving and incoming groups in the apical positions. Calculations as described above using the Pauling formula indicate that the shorter separation of leaving and incoming oxygens (4.6 Å) represents a reaction with approximately 11% associative character. The cAPK kinase, like phosphorylase kinase, contains two metal ions at the catalytic site. Two of the fluorine atoms coordinate with the Mg^{2+} ions, and one of them also interacts with the catalytic site lysine. A third fluorine interacts with the amide nitrogen of Ser53 from the glycine loop. These represent slightly more extensive interactions than those seen in the present pCDK2/cyclin A complex with nitrate, especially those generated by the second metal site. The interactions could explain the apparent higher degree of associative character of the cAPK reaction than that suggested by the present structural studies with pCDK2/cyclin A.

ACKNOWLEDGMENT

We are grateful for the support of the beam line scientists at ID14.1, ESRF, at Elettra, and at SRS. We thank our colleagues Nick Brown and Robert Chang for preparation of the pCDK2/cyclin A crystals and Martin Noble for help with data collection, advice on refinement, and the use of AESOP. We also thank Magda Kosmopoulou for help in the kinetic experiments.

REFERENCES

1. Morgan, D. O. (1997) *Annu. Rev. Cell Dev. Biol. 13*, 261−291.
2. Johnson, L. N., and Lewis, R. J. (2001) *Chem. Rev. 101*, 2209−2242.
3. Schindler, T., Bornmann, W., Pellicena, P., Miller, W. T., Clarkson, B., and Kuriyan, J. (2000) *Science 289*, 1938−1942.
4. Knighton, D. R., Zheng, J., Eyck, L. F. T., Xuong, N., Taylor, S. S., and Sowadski, J. M. (1991) *Science 253*, 414−420.
5. Bossmeyer, D., Engh, R. A., Kinzel, V., Ponstingl, H., and Huber, R. (1993) *EMBO J. 12*, 849−859.
6. Hubbard, S. R. (1997) *EMBO J. 16*, 5572−5581.
7. Lowe, E. D., Noble, M. E. M., Skamnaki, V. T., Oikonomakos, N. G., Owen, D. J., and Johnson, L. N. (1997) *EMBO J. 16*, 6646−6658.
8. Brown, N. R., Noble, M. E. M., Endicott, J. A., and Johnson, L. N. (1999) *Nat. Cell Biol. 1*, 438−443.
9. Jeffrey, P. D., Russo, A. A., Polyak, K., Gibbs, E., Hurwitz, J., Massague, J., and Pavletich, N. P. (1995) *Nature 376*, 313−320.
10. Russo, A., Jeffrey, P. D., and Pavletich, N. P. (1996) *Nat. Struct. Biol. 3*, 696−700.
11. Hagopian, J. C., Kirtley, M. P., Stevenson, L. M., Gergis, R. M., Russo, A. A., Pavletich, N. P., Parsons, S. M., and Lew, J. (2001) *J. Biol. Chem. 276*, 275−280.
12. Adams, J. A., and Taylor, S. S. (1992) *Biochemistry 31*, 8516−8522.
13. Grant, B. D., and Adams, J. A. (1996) *Biochemistry 35*, 2022−2029.
14. Skamnaki, V. T., Owen, D. J., Noble, M. E. M., Lowe, E. D., Lowe, G., Oikonomakos, N. G., and Johnson, L. N. (1999) *Biochemistry 38*, 14718−14730.
15. Knowles, J. R. (1980) *Annu. Rev. Biochem. 49*, 877−919.
16. Admiraal, S. J., and Herschlag, D. (1995) *Chem. Biol. 2*, 729−739.
17. Mildvan, A. S. (1997) *Proteins: Struct., Funct., Genet. 29*, 401−416.
18. Schlichting, I., and Reinstein, J. (1997) *Biochemistry 36*, 9290−9296.
19. Xu, Y.-W., Morera, S., Janin, J., and Cherfils, J. (1997) *Proc. Natl. Acad. Sci. U.S.A. 94*, 3579−3583.
20. Braig, K., Menz, R. I., Montgomery, M. G., Leslie, A. G. W., and Walker, J. E. (2000) *Structure 8*, 567−573.
21. Scheffzek, K., Ahmadian, M. R., Kabsch, W., Wiesmuller, L., Lautwein, A., Schmitz, F., and Wittinghofer, A. (1997) *Science 277*, 333−338.
22. Zhou, G., Somasundaram, T., Blanc, E., Parthasarathy, G., Ellington, W. R., and Chapman, M. S. (1998) *Proc. Natl. Acad. Sci. U.S.A. 95*, 8449−8454.
23. Ablooglu, A. J., Till, J. H., Kim, K., Parang, K., Cole, P. A., Hubbard, S. R., and Kohanski, R. A. (2000) *J. Biol. Chem. 275*, 30394−30398.
24. Kim, K., and Cole, P. A. (1998) *J. Am. Chem. Soc. 120*, 6851−6858.
25. Parang, K., Till, J. H., Ablooglu, A. J., Kohanski, R. A., Hubbard, S. R., and Cole, P. A. (2001) *Nat. Struct. Biol. 8*, 37−41.
26. Schlichting, I., and Reinstein, J. (1999) *Nat. Struct. Biol. 6*, 721−723.
27. Gresser, M. J., and Tracey, A. S. (1990) in *Vanadium in Biological Systems: Physiology and Biology* (Chasten, D. N., Ed.) pp 63−90, Kluwer, Amsterdam.
28. Pannifer, A. D. B., Flint, A. J., Tonks, N. K., and Barford, D. (1998) *J. Biol. Chem. 273*, 10454−10462.
29. Wlodawer, A., Miller, M., and Sjolin, L. (1983) *Proc. Natl. Acad. Sci. U.S.A. 80*, 3628−3631.
30. Smith, C. A., and Rayment, I. (1996) *Biochemistry 35*, 5404−5417.
31. Collaborative Computational Project No. 4 (1994) *Acta Crystallogr. D50*, 760−763.
32. Murshudov, G. N., Vagen, A. A., and Dodson, E. J. (1997) *Acta Crystallogr. D53*, 240−255.
33. Read, R. J. (1986) *Acta Crystallogr. A42*, 140−149.
34. Jones, T. A., Zou, J. Y., Cowan, S. W., and Kjeldgaard, M. (1991) *Acta Crystallogr. A47*, 110−119.

35. Lamzin, V. S., and Wilson, K. S. (1993) *Acta Crystallogr. D49*, 129−147.
36. Cook, F. N., Neville, M. E., Vrana, K. E., Hartl, F. T., and Roskowski, R. (1982) *Biochemistry 21*, 5794−5799.
37. Adams, J. A., McGlone, M. L., Gibson, R., and Taylor, S. S. (1995) *Biochemistry 34*, 2447−2454.
38. Owen, D. J., Papageorgiou, A. C., Garman, E. F., Noble, M. E. M., and Johnson, L. N. (1995) *J. Mol. Biol. 246*, 376−383.
39. Helmreich, E. J. M., and Cori, C. F. (1964) *Proc. Natl. Acad. Sci. U.S.A. 51*, 131−138.
40. Fischer, E. H., and Krebs, E. G. (1962) *Methods Enzymol. 5*, 369−372.
41. Melpidou, A. E., and Oikonomakos, N. G. (1983) *FEBS Lett. 154*, 105−110.
42. Kastenscmidt, L. L., Kastenschmidt, J., and Helmreich, E. J. M. (1968) *Biochemistry 7*, 3590−3608.
43. Bradford, M. M. (1976) *Anal. Biochem. 72*, 248−254.
44. Leatherbarrow, R. J. (1992) *GrafFit*, version 3.0, Erithacus Software, Staines, U.K.
45. Gordon, A. J. (1991) *Methods Enzymol. 5*, 369−373.
46. Armstrong, R. N., Kondo, H., Granot, J., Kaiser, E. T., and Mildvan, A. S. (1979) *Biochemistry 18*, 1230−1238.
47. Zheng, J., Knighton, D. R., Eyck, L. F. T., Karlsson, R., Xuong, N., Taylor, S. S., and Sowadski, J. M. (1993) *Biochemistry 32*, 2154−2161.
48. Adams, J. A., and Taylor, S. S. (1993) *Protein Sci. 2*, 2177−2186.
49. Madhusudan, Akamine, P., Xuong, N.-X., and Taylor, S. S. (2002) *Nat. Struct. Biol. 9*, 273−277.

BI0201724